First-principles study on the optical properties for CsI crystal with a pair of V_{Cs}^{1-}-V_{I}^{1+}

Tingyu Liu (刘廷禹)[1,2*], Feinan Yan (严非男)[1,2], Jun Chen (陈 俊)[1,2], and Liping Liang (梁丽萍)[1,2]

[1] *College of Science, University of Shanghai for Science and Technology, Shanghai 200093, China*

[2] *Shanghai Key Laboratory of Contemporary Optics System, Shanghai 200093, China*

[*] *E-mail: liutyyxj@163.com*

Received March 16, 2009

The electronic structures and optical properties of both the perfect CsI crystal and the crystal containing a pair of V_{Cs}^{1-}-V_{I}^{1+} are calculated using CASTEP code with the lattice structure optimized. The calculated results indicate that the optical symmetry of the CsI crystal coincides with the lattice structure geometry of the CsI crystal. The absorption spectrum of the CsI crystal containing a pair of V_{Cs}^{1-}-V_{I}^{1+} also does not occur in the visible and near-ultraviolet range. It reveals that the existence of the pair of V_{Cs}^{1-}-V_{I}^{1+} in CsI crystal has no visible effects on the optical properties of the CsI crystal.

OCIS codes: 160.4670, 160.2220, 160.4760.

doi: 10.3788/COL20100801.0074.

Cesium iodide crystal is widely used as a scintillator material in particle detectors due to its high emission efficiency and fast decay time, especially the crystal doped with thallium[1−4]. In general, this kind of simple cubic structured crystal would be easily damaged by high-energy irradiation, such as X- or γ-ray, resulting in the creation of color centers and making the crystal occur absorption bands in the visible range.

The Kr ion irradiated CsI[5] exhibits several absorption bands peaking at 240, 335, 410, 560, and 751 nm with a shoulder at 716 nm. The absorption bands of color centers are harmful to the scintillate properties. Many researchers have discussed the origins of these absorption bands[5−8]. The CsI crystal after the irradiation exhibits six absorption bands peaking at 375, 560, 750, 1020, 1180, and 285 nm[9]. The former five bands are assigned to I_2^{1-} color center, H band, F band, I_3^{2-} color center, and F_2 color center, respectively. The origin of the absorption band at 285 nm is still unclear[9]. The growth of optical absorption spectra in a high-Tl crystal over a wide range of γ-ray dose show a group of six peaks, which are at 355, 390, 430, 460, 520, and 560 nm. In the infrared region, 840-nm absorption band originating from the F-band and 980-nm absorption band related to the F_3-band are also observed[10]. The short wavelength absorption bands are generally assigned to V band and the long wavelength absorption bands are assigned to F bands[6].

On the other hand, there are a large number of successful simulations on the optical properties of crystals using the density functional theory (DFT)[11,12] with the code called CASTEP. In order to further study the physical properties of the pair of V_{Cs}^{1-}-V_{I}^{1+} related defects, the electronic structures, dielectric function, complex refractive index, and absorption spectra of both the perfect CsI cluster and the CsI cluster containing a pair of V_{Cs}^{1-}-V_{I}^{1+} under the irradiation of a polarized light are calculated using CASTEP code with the lattice structure optimized. The lattice structure optimization is required before we study the optical properties of the crystal due to the lattice distortion caused by the existence of V_{Cs}^{1-}-V_{I}^{1+}.

The CsI single crystal is simple cubic structured. The CsI supercell used here consists of 27 Cs and 27 I centered at I, having the chemical formula of $[Cs_{27}I_{27}]$. The CsI supercell containing a pair of V_{Cs}^{1-}-V_{I}^{1+} has a Cs vacancy V_{Cs}^{1-} nearest centered I ion and an iodine V_{I}^{1+} replacing the centered I^{1-} ions.

The CASTEP code is used for the lattice optimization for the CsI containing one or two vacancies and the calculation of the ground-state electronic structure using a plane-wave pseudo-potential formulation within the framework of DFT with generalized gradient correction in the form of PW91[13−15]. We use ultrasoft pseudopotentials for the iodine and cesium atoms and a plane-wave cutoff energy of 340 eV. The basic parameters are chosen as follows: kinetic energy cutoff of 340 eV, fast Fourier transform (FFT) grid dimensions of 60×60×64, space representation being reciprocal, and self-consistent field (SCF) tolerance 1.0×10^{-6} of eV/atom. Optimal atomic positions are determined until satisfying the conditions: 1) the maximal force on them is smaller than 0.5 eV/nm; 2) the maximal change of energy per atom is smaller than 0.00001 eV; and 3) the maximal displacement is smaller than 0.0001 nm. All other calculations are performed on basis of the lattice structure being optimized.

The dielectric function of an anisotropic material is a complex symmetric second-order tensor which describes the linear response of an electronic system to an applied external electric field. The imaginary part of the dielectric tensor is directly related to the electronic band structure of a solid, so it can be computed from the knowledge of single-particle orbitals and energies approximated by the solutions of the Kohn-Sham equations. However, it is a well known fact that DFT calculations underestimate the band gap. To take this into account, a 'scissors operator' is used, allowing a shift of the bands situated above the valence band and a rescaling of the matrix elements.

Hence, assuming the one-electron rigid band approximation, neglecting electron polarization effects (Koopmans' approximation), and in the limits of linear optics and the visible-ultraviolet region, the imaginary part of the dielectric tensor is given by[16,17]

$$\varepsilon_{\mathrm{i}}(\omega)=\frac{e^2\pi^2}{\varepsilon_0 m^2(\omega-\Delta c/\hbar)^2}\sum_{\mathrm{V,C}}\left\{\int_{\mathrm{BZ}}\frac{2\mathrm{d}\vec{K}}{(2\pi)^3}\left|\vec{a}\cdot\vec{M}_{\mathrm{V,C}}\right|^2\delta\left[E_{\mathrm{C}}\left(\vec{K}\right)+\Delta c-E_{\mathrm{V}}\left(\vec{K}\right)-\hbar\omega\right]\right\},\tag{1}$$

where $\vec{a}$ is the unit vector potential, $\vec{M}_{\mathrm{v,c}}$ is the matrix of dipole transition, subscript "C" means the conduction band, "V" means the valence band, BZ is the Brillouin zone, Δc is the shifting value of the scissors operator, e is the electron charge, ε_0 is the dielectric constant in vacuum, m is the free electron mass, ω is the frequency of the incident wave, $\hbar$ is the Planck constant, and $\vec{K}$ is the wave vector. The Kramers-Kröning transformation links the real and the imaginary parts of the dielectric function. The Kramers-Kröning transformation and the smearing factor of 0.12 eV are used to obtain the real part $\varepsilon_{\mathrm{r}}(\omega)$ of the dielectric function. According to the fact that the calculated band gap of the perfect CsI crystal is 4.7 eV and the experimental value is 6.2 eV, the shifting value of the scissors operator Δc is chosen as 1.5 eV. For dielectric tensor calculation, the BZ integration is made with 64 independent k-points for CsI crystal.

The electronic structures are calculated in the range between −30 and 10 eV. The total densities of states (TDOS) for the perfect CsI crystal are plotted in Fig. 1 in comparison with those for the CsI crystal containing a pair of V_{Cs}^{1-}-V_I^{1+}. In this letter, all the curves related to the perfect CsI crystal are plotted in dotted lines and those related to the CsI containing a pair of V_{Cs}^{1-}-V_I^{1+} are plotted in solid lines. It can be seen from Fig. 1 that the TDOS of the perfect CsI crystal exhibits seven peaks located at −20.5, −10.5, −7.2, −0.84, −0.1, 6.2, and 6.8 eV, corresponding to Cs 5s, I 5s, Cs 5p, I 5p, I 5p, Cs 5d, and I 5d, respectively. The top of the valence band is mainly composed of 5p state of iodine. Different from the results given by Satpathy *et al.*[18,19], the I 5p state is split into two peaks only. The same result can be obtained using the *ab inition* study[20]. The bottom of the conduction band is mainly composed of the Cs 5d state. Our calculated results are in good agreement with those published in Ref. [21].

Compared with the perfect CsI crystal, the TDOS of CsI crystal containing a pair of V_{Cs}^{1-}-V_I^{1+} in the regions below Fermi level is quite similar to that for perfect CsI crystal. It means that the existence of the pair of V_{Cs}^{1-}-V_I^{1+} has few effects on the valance band and the core electrons of the ions in the crystal. A new additional small peak located at 5.2 eV appears in the CsI crystal containing a pair of V_{Cs}^{1-}-V_I^{1+}. The existence of the pair of V_{Cs}^{1-}-V_I^{1+} causes a reduction of the band gap about 1.0 eV.

The frequency-dependent dielectric functions ε_{i} and ε_{r} have been calculated. Figure 2 shows the calculated imaginary part of the dielectric function for polarized light with the electrical vector $\vec{E}$ parallel to axes $\vec{a}$, $\vec{b}$, and $\vec{c}$ (marked as $\vec{E}//\vec{a}$, $\vec{E}//\vec{b}$, and $\vec{E}//\vec{c}$), respectively. It can be seen that, for the perfect CsI crystal, the imaginary part of the dielectric function occurs isotropy, while for CsI crystal containing a pair of V_{Cs}^{1-}-V_I^{1+}, there is a minute difference. This is because that the lattice symmetry is slightly destroyed by the existence of the pair of V_{Cs}^{1-}-V_I^{1+}. This difference will not be further discussed here since it is almost invisible. The symmetry of the imaginary part of the dielectric function implies

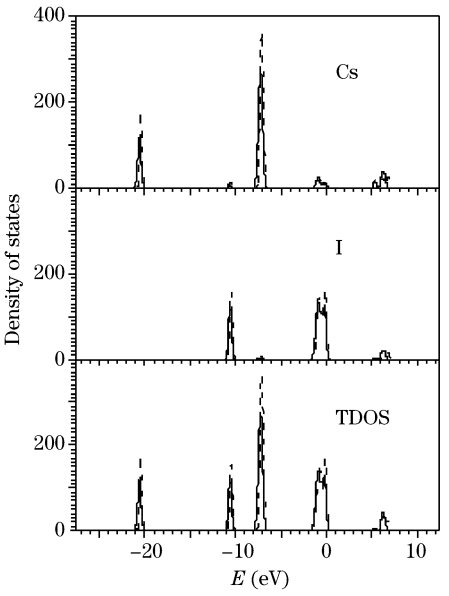

Fig. 1. TDOS of the perfect CsI crystal (dotted lines) and the CsI crystal containing a pair of V_{Cs}^{1-}-V_I^{1+} (solid lines).

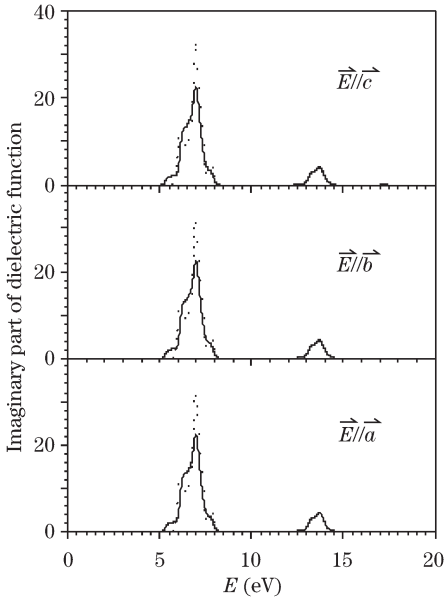

Fig. 2. Imaginary parts of the dielectric function for the perfect CsI crystal (dotted lines) and the CsI crystal containing a pair of V_{Cs}^{1-}-V_I^{1+} (solid lines).

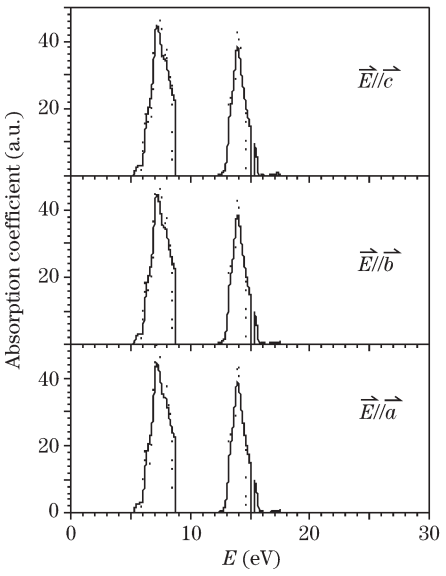

Fig. 3. Absorption spectra of the perfect CsI crystal (dotted lines) and CsI crystal containing a pair of V_{Cs}^{1-}-V_I^{1+} (solid lines) in irradiation of a polarized light with $\vec{E}//\vec{a}$, $\vec{E}//\vec{b}$, and $\vec{E}//\vec{c}$.

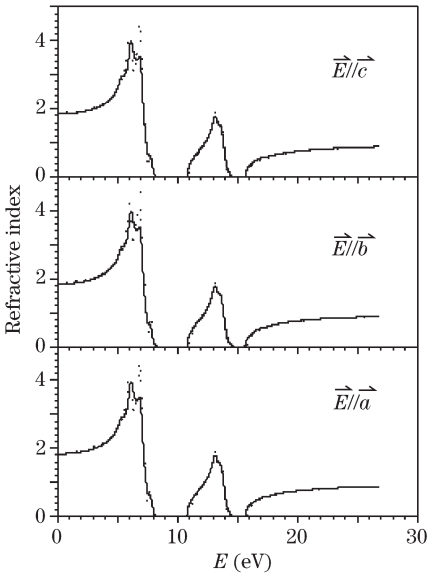

Fig. 4. Refractive indices of the CsI crystal (dotted lines) and CsI crystal containing a pair of V_{Cs}^{1-}-V_I^{1+} (solid lines) in irradiation of a polarized light with $\vec{E}//\vec{a}$, $\vec{E}//\vec{b}$, and $\vec{E}//\vec{c}$.

the symmetry of the lattice structure.

The imaginary part spectra of the dielectric function of the perfect CsI exhibit seven peaks located at 6.20, 6.95, 7.41, 7.88, 13.20, and 13.9 eV, respectively, and tend to zero below 6.0 eV. Compared with the perfect CsI crystal, the spectra of the imaginary part of the dielectric function for the CsI containing a pair of V_{Cs}^{1-}-V_I^{1+} exhibit a new small peak located at 5.50 eV, which is related to the new state peak located at 5.2 eV.

The absorption coefficient follows the relationship $\sigma = \dfrac{\omega\varepsilon_i}{nc}$. The absorption spectra under $\vec{E}//\vec{a}$, $\vec{E}//\vec{b}$, and $\vec{E}//\vec{c}$ calculated from the perfect CsI crystal and the CsI crystal containing a pair of V_{Cs}^{1-}-V_I^{1+} are shown in Fig. 3. For the perfect CsI crystal, there is no absorption in the visible and near-ultraviolet region. This means that the perfect CsI should be a transparent crystal. There are eight peaks of absorption band under $\vec{E}//\vec{a}$, and $\vec{E}//\vec{b}$ in the range between 6.0 and 16 eV located at 6.18, 7.00, 7.40, 7.90, 13.30, and 13.9 eV, corresponding to the transitions of the electron from the states distributed in the valence band to the bottom of the conduct band. For example, the peak at 6.18 eV is attributed to the electronic transition from the state peaking at −0.10 eV in the valence band to the bottom of the conduct band.

Compared with the spectra of the perfect CsI crystal shown in Fig. 3, the absorption spectra for the CsI containing a pair of V_{Cs}^{1-}-V_I^{1+} show that the absorption spectrum occurs two new absorption bands locating at about 5.5 and 15.4 eV, and there does not exist a new band in the visible and near-ultraviolet region. It means that the existence of the pair of V_{Cs}^{1-}-V_I^{1+} has no visible effect on the absorption spectra.

The refractive index and the extinctive coefficient follow the relationship $n^2 - \kappa^2 = \varepsilon_r$ and $2n\kappa = \varepsilon_i$. The numerical results are shown in Fig. 4. Same as the results on absorption spectra and the imaginary part of the dielectric function, the refractive index has the structure of five peaks. The peaks are located at 5.96, 6.85, 7.74, 13.08, and 13.64 eV, respectively. The calculated result is in good agreement with the experimental results (n = 1.78) in the visible region[22]. The polarization properties of the refractive index are also similar to those of the imaginary part of the dielectric function and the absorption bands, which implies the inherent relationship of the three physical quantities.

In conclusion, the electronic structure, dielectric function, complex refractive index, and absorption spectra of the perfect CsI crystal and the CsI crystal containing a pair of V_{Cs}^{1-}-V_I^{1+} have been calculated using the CASTEP code. A polarized light is used with its electric vector $\vec{E}$ parallel to the axis $\vec{a}$, $\vec{b}$, and $\vec{c}$, respectively. Variant electronic transitions between the states distributed in the valence band to the bottom of conduct band, corresponding to the peaks in optical properties such as the dielectric function and refractive index, have been studied in detail. It is found that the CsI crystal containing a pair of V_{Cs}^{1-}-V_I^{1+} does not occur absorption band in the visible and near-ultraviolet range.

This work was supported by the Foundation of Shanghai Municipal Education Committee, China (No. 09YZ210), the Shanghai Leading Academic Discipline Project (No. S30502), and the Program from Shanghai Commitee of Science and Technology (No. 07DZ22026)

References

1. C. Regenfus, C. Amsler, A. Glauser, D. Grögler, D. Lindelöf, and H. Pruys, Nucl. Instr. Methods Phys. Res. A **504,** 343 (2003).
2. P. F. Bloser, J. M. Ryan, M. L. McConnell, J. R. Macri, R. Andritschke, G. Kanbach, and A. Zoglauer, New Astron. Rev. **50,** 619 (2006).
3. M. Doroshenko, K. Abe, J. K. Ahn, Y. Akune, V. Bara-

nov, Y. Fujioka, Y. B. Hsiung, T. Ikeif, T. Inagaki, S. Ishibashi, H. Ishii, T. Iwata, S. Kobayashi, S. Komatsu, T. K. Komatsubara, A. Kurilin, E. Kuzmin, A. Lednev, H. S. Lee, S. Y. Lee, G. Y. Lim, T. Matsumura, T. Mizuhashi, A. Moisseenko, T. Morimoto, T. Nakano, N. Nishi, J. Nix, T. Nomura, T. Oba, H. Okuno, K. Omata, G. N. Perdue, S. Perov, S. Podolsky, S. Porokhovoy, K. Sakashita, N. Sasao, H. Sato, T. Sato, M. Sekimoto, T. Shinkawa, Y. Sugaya, A. Sugiyama, T. Sumida, Y. Tajima, Z. Tsamalaidze, T. Tsukamoto, Y. Wah, H. Watanabe, M. Yamaga, T. Yamanaka, H. Y. Yoshida, and Y. Yoshimura, Nucl. Instr. Methods Phys. Res. A **545,** 278 (2005).

4. M. Marisaldi, C. Fiorini, C. Labanti, A. Longoni, F. Perotti, E. Rossi, and H. Soltau, Nucl. Phys. B **150,** 190 (2006).
5. A. I. Popov and E. Balanzat, Nucl. Instr. Methods Phys. Res. B **166-167,** 545 (2000).
6. G. O. Amolo, R. M. Erasmus, J. D. Comins, and T. E. Derry, Nucl. Instr. Methods Phys. Res. B **250,** 359 (2006).
7. D. W. Lynch, A. D. Brothers, and D. A. Robinson, Phys. Rev. **139,** A285 (1965).
8. P. Avakian and A. Smakula, Phys. Rev. **120,** 2007 (1960).
9. M. Okada, M. Nakagawa, K. Atobe, N. Itatani, and K. Ozawa, Phys. Stat. Sol. (a) **167,** 253 (1998).
10. M. A. H. Chowdhury, A. Holmes-Siedle, A. K. McKemey, S. J. Watts, and D. C. Imrie, Nucl. Instr. Methods Phys. Res. A **413,** (1998).
11. L. Feng, Z. Liu, and B. Xu, Acta Opt. Sin. (in Chinese) **28,** 2191 (2008).
12. Q. Hou, Y. Zhang, and T. Zhang, Acta Opt. Sin. (in Chinese) **28,** 1347 (2007).
13. A. E. Mattsson, R. Armiento, P. A. Schultz, and T. R. Mattsson, Phys. Rev. B **73,** 195123 (2006).
14. S. Sharma, T. Nautiyal, G. S. Singh, S. Auluck, P. Blaha, and C. Ambrosch-Draxl, Phys. Rev. B **59,** 14833 (1999).
15. F. Goubin, Y. Montardi, P. Deniard, X. Rocquefelte, R. Brec, and S. Jobic, J. Solid State Chem. **177,** 89 (2004).
16. R. Fang, *Spectroscopy of Solid* (University of Science and Technology of China Press, Hefei, 2001).
17. Y. Abraham, N. A. Holzwarth, and R. T. Williams, Phys. Rev. B **62,** 1733 (2000).
18. S. Satpathy, Phys. Rev. B **33,** 8706 (1986).
19. S. Satpathy, N. E. Christensen, and O. Jepsen, Phys. Rev. B **32,** 6793 (1985).
20. R. M. Ribeiro, J. Coutinho, V. J. B. Torres, R. Jones, S. J. Sque, S. Öberg, M. J. Shaw, and P. R. Briddon, Phys. Rev. B **74,** 035430 (2006).
21. A. Yu. Kuznetsov, A. B. Sobolev, A. S. Makarov, and A. N. Velichko, Phys. Solid State **47,** 1950 (2005).
22. M. Saito and T. Yasuda, Appl. Opt. **42,** 2366 (2003).